Investigation of the ellipsoidal-statistical Bhatnagar–Gross–Krook kinetic model applied to gas-phase transport of heat and tangential momentum between parallel walls

M. A. Gallis[a] and J. R. Torczynski
Engineering Sciences Center, Sandia National Laboratories, Albuquerque, New Mexico 87185-0346, USA

(Received 15 September 2010; accepted 17 January 2011; published online 1 March 2011)

The ellipsoidal-statistical Bhatnagar–Gross–Krook (ES-BGK) kinetic model is investigated for steady gas-phase transport of heat, tangential momentum, and mass between parallel walls (i.e., Fourier, Couette, and Fickian flows). This investigation extends the original study of Cercignani and Tironi, who first applied the ES-BGK model to heat transport (i.e., Fourier flow) shortly after this model was proposed by Holway. The ES-BGK model is implemented in a molecular-gas-dynamics code so that results from this model can be compared directly to results from the full Boltzmann collision term, as computed by the same code with the direct simulation Monte Carlo (DSMC) algorithm of Bird. A gas of monatomic molecules is considered. These molecules collide in a pairwise fashion according to either the Maxwell or the hard-sphere interaction and reflect from the walls according to the Cercignani–Lampis–Lord model with unity accommodation coefficients. Simulations are performed at pressures from near-free-molecular to near-continuum. Unlike the BGK model, the ES-BGK model produces heat-flux and shear-stress values that both agree closely with the DSMC values at all pressures. However, for both interactions, the ES-BGK model produces molecular-velocity-distribution functions that are qualitatively similar to those determined for the Maxwell interaction from Chapman–Enskog theory for small wall temperature differences and moment-hierarchy theory for large wall temperature differences. Moreover, the ES-BGK model does not produce accurate values of the mass self-diffusion coefficient for either interaction. Nevertheless, given its reasonable accuracy for heat and tangential-momentum transport, its sound theoretical foundation (it obeys the H-theorem), and its available extension to polyatomic molecules, the ES-BGK model may be a useful method for simulating certain classes of single-species noncontinuum gas flows, as Cercignani suggested. © *2011 American Institute of Physics*. [doi:10.1063/1.3558869]

I. INTRODUCTION

The complicated structure of the term that represents collisions between gas molecules makes the Boltzmann equation, which describes noncontinuum gas dynamics, difficult to solve. Cercignani[1] outlined one approach to dealing with this issue that was first suggested during the earliest investigations involving the Boltzmann equation and is still used at the present time:

"It is therefore not surprising that alternative, simpler expressions have been proposed for the collision term; they are known as collision models, and any Boltzmann-like equation where the Boltzmann collision integral is replaced by a collision model is called a model equation or a kinetic model. The idea behind this replacement is that a large amount of detail of the two-body interaction (which is contained in the collision term) is not likely to influence significantly the values of many experimentally measured quantities."

Thus, kinetic models have the potential to produce reasonably accurate values for macroscopic quantities such as number density, velocity, pressure, temperature, heat flux, and shear stress. Additionally, Cercignani noted that kinetic models offer the possibility of obtaining analytical results that cannot be obtained with the Boltzmann collision term.[1] However, these advantages come at a price: Kinetic models may not represent the molecular velocity distribution as accurately as the Boltzmann collision term. Therefore, the accuracy of kinetic models continues to remain a subject of investigation.[2]

In a pioneering paper, Bhatnagar, Gross, and Krook (BGK) developed a kinetic model in which the Boltzmann collision term is replaced with a much simpler but nonlinear form involving a Maxwellian distribution at local conditions.[3] The BGK model, however, has a serious drawback in that it produces a Prandtl number of unity rather than a value around 2/3, as observed for monatomic gases.[4] To overcome this defect, Holway replaced the local Maxwellian distribution with a local ellipsoidal-statistical (ES) distribution, and the resulting ES-BGK kinetic model reproduces the desired Prandtl number.[5–7] Unlike the BGK model, it was not initially obvious that the ES-BGK model ultimately leads to the equilibrium state. However, Andries and co-workers placed the ES-BGK model on a firm theoretical foundation by proving that it obeys the H-theorem.[8–10] The ES-BGK model has been extended from single-species monatomic

[a]Author to whom correspondence should be addressed. Tel.: 505-844-7639. FAX: 505-844-6620. Electronic mail: magalli@sandia.gov.

gases to gas mixtures and to gases with polyatomic molecules (i.e., having internal energy).[5–10]

Although most investigators focused on applying the BGK and ES-BGK kinetic models to shock-wave structure,[6,11–13] Cercignani and Tironi[14] were the first to recognize the usefulness of wall-bounded noncontinuum gas flows for investigating the accuracy of the ES-BGK kinetic model. More specifically, they analyzed heat transfer in a gas between parallel walls at fixed temperatures (i.e., Fourier flow) and determined the temperature profiles and the corresponding heat fluxes for several values of the system Knudsen number and the ratio of the wall temperatures. Encouraged by such results, other investigators have investigated using the ES-BGK kinetic model for diverse applications, including gas damping of oscillating microbeams,[15] low-pressure shock tubes,[16] spacecraft re-entry flows,[17] and radiometer vanes.[18]

Given its success in reproducing macroscopic quantities, it is appropriate to investigate the accuracy of the ES-BGK kinetic model for the molecular velocity distribution itself. Garzó and Santos considered the Boltzmann collision term, the BGK model, and the ES-BGK model (which they refer to as "Gaussian") and compared high-order moments of the molecular-velocity-distribution function for uniform shear flow, a mathematically tractable analog to gas between oppositely sliding walls (i.e., Couette flow).[19,20] Surprisingly, they found that the BGK results were closer to the Boltzmann results than the ES-BGK results were in almost all cases.

In the remaining sections, results from using the ES-BGK and BGK kinetic models are compared to corresponding results from using the Boltzmann collision term for Fourier flow, Couette flow, combined Fourier–Couette flow, and Fickian diffusion. The Boltzmann collision term is computed using a molecular-gas-dynamics (MGD) code that implements the direct simulation Monte Carlo (DSMC) method of Bird.[21] Wagner proved that solutions obtained using the DSMC method approach solutions of the Boltzmann equation for a monatomic gas in the limit of vanishing discretization and stochastic errors,[22] and Gallis and co-workers demonstrated that the DSMC method accurately reproduces the results of Chapman–Enskog (CE) theory in the continuum limit.[23–26]

The ES-BGK and BGK kinetic models are implemented in the same MGD code simply by modifying the algorithm for molecular collisions: The algorithms for molecular motion[21] and for reflection from solid boundaries[27–29] are unchanged. Molecular-velocity-distribution results are obtained for these kinetic models and are compared to theoretical results based on CE theory for Maxwell and hard-sphere molecular interactions, to moment-hierarchy (MH) theory for Maxwell molecular interactions, and to computational results based on DSMC simulations for both interactions.[23–26] The ES-BGK kinetic model is seen to produce accurate values of quantities such as the heat flux and the shear stress but to produce molecular-velocity-distribution functions that are only qualitatively similar to those produced by the Boltzmann collision term. Moreover, the ES-BGK kinetic model fails to produce accurate values of the self-diffusion coefficient for either interaction.

II. THEORETICAL CONSIDERATIONS

A. Boltzmann equation

The molecular-velocity-distribution function f provides a complete description of a dilute monatomic gas at the molecular level.[4] The expected number of molecules with positions within volume $d\mathbf{x}$ centered at position $\mathbf{x}$ and with velocities within velocity volume $d\mathbf{v}$ centered at velocity $\mathbf{v}$ at time t is given by $f[t,\mathbf{x},\mathbf{v}]d\mathbf{x}d\mathbf{v}$. Macroscopic quantities such as the number density n, the average velocity $\mathbf{u}$, and the temperature T are found in terms of moments of f, which are sometimes expressed more conveniently in terms of the thermal (peculiar) molecular velocity $\mathbf{c}=\mathbf{v}-\mathbf{u}$:

$$n\{1,\mathbf{u},3k_BT\}=\int\{1,\mathbf{v},m|\mathbf{c}|^2\}fd\mathbf{v}. \tag{1}$$

Here, m is the molecular mass, and k_B is the Boltzmann constant.

The Boltzmann equation expresses the relationship between the molecular-velocity-distribution function and the variables on which it depends:[4]

$$\frac{\partial f}{\partial t}+\mathbf{v}\cdot\frac{\partial f}{\partial \mathbf{x}}+\frac{\mathbf{F}}{m}\cdot\frac{\partial f}{\partial \mathbf{v}}=\left[\frac{\partial f}{\partial t}\right]_{\text{coll}}. \tag{2}$$

Here, $\mathbf{F}$ is any (velocity-independent) external force, and the right side of the equation is the Boltzmann collision term:[4]

$$\left[\frac{\partial f}{\partial t}\right]_{\text{coll}}=\int_{-\infty}^{\infty}\int_{0}^{4\pi}(f^*f_1^*-ff_1)|\mathbf{v}-\mathbf{v}_1|\sigma d\Omega d\mathbf{v}_1. \tag{3}$$

In the collision-term integral, the distribution functions f and f^* are evaluated at the molecule's precollision velocity $\mathbf{v}$ and postcollision velocity $\mathbf{v}^*$, respectively; the distribution functions f_1 and f_1^* are evaluated at the collision partner's precollision velocity $\mathbf{v}_1$ and postcollision velocity $\mathbf{v}_1^*$, respectively; Ω is the solid angle; and σ is the collision cross section, which contains information about the molecular interaction (e.g., Maxwell or hard sphere). The complicated structure of the Boltzmann collision term has made analysis and application of the Boltzmann equation difficult.

B. BGK collision-term model

Bhatnagar *et al.* suggested replacing the complicated Boltzmann collision term with a simpler form, now called the BGK kinetic model:[3]

$$\left[\frac{\partial f}{\partial t}\right]_{\text{BGK}}=\nu(f_M-f). \tag{4}$$

Here, f_M is the Maxwellian distribution corresponding to the local values of the number density, the temperature, and the average velocity, and ν is the relaxation rate, which does not depend on the molecular velocity. The BGK model reproduces the correct Maxwellian distribution at equilibrium, preserves conservation of mass, momentum, and energy, sat-

isfies the H-theorem, and leads to the Navier–Stokes equations when the Chapman–Enskog expansion is applied.[4]

The BGK relaxation rate ν determines the viscosity μ and the thermal conductivity K according to the following expressions, where C_p is the specific heat at constant pressure:[4]

$$\mu = \frac{nk_BT}{\nu}, \tag{5}$$

$$K = C_p\frac{nk_BT}{\nu}, \tag{6}$$

$$C_p = \frac{5}{2}\frac{k_B}{m}. \tag{7}$$

These expressions lead to a Prandtl number of $\mathrm{Pr}=\mu C_p/K=1$, whereas actual monatomic gases have Prandtl numbers of $\mathrm{Pr}\approx 2/3$. In other words, the BGK kinetic model can reproduce either the viscosity or the thermal conductivity of a monatomic gas but not both simultaneously. As a result, the BGK kinetic model is generally restricted either to situations with temperature variations but without motion (e.g., Fourier flow) or to situations with motion but without temperature variations (e.g., Couette flow in the low-speed limit). In the former situation, Eq. (6) is used to prescribe the relaxation rate ν, and the model is referred to as BGK-K (thermal conductivity). In the latter situation, Eq. (5) is used to prescribe the relaxation rate ν, and the model is referred to as BGK-μ (viscosity).

C. ES-BGK collision-term model

Holway modified the BGK kinetic model by replacing the equilibrium Maxwellian distribution with the ES distribution.[5–7] The ES-BGK model is expressed below using equivalent notation that emphasizes its relationship to the BGK model:[13]

$$\left[\frac{\partial f}{\partial t}\right]_{\text{ES-BGK}} = \nu(f_{\text{ES}} - f), \tag{8}$$

$$f_{\text{ES}} = \frac{n}{\det[\mathbf{S}]}\left(\frac{m}{2\pi k_BT}\right)^{3/2}\exp\left[-\frac{m\mathbf{C}^{\mathrm{T}}\mathbf{C}}{2k_BT}\right], \tag{9}$$

$$\mathbf{c} = \mathbf{SC}, \tag{10}$$

$$\mathbf{SS} = \mathbf{I} - \frac{1-\mathrm{Pr}}{\mathrm{Pr}}\left(\frac{3\mathbf{P}}{\mathrm{trace}[\mathbf{P}]} - \mathbf{I}\right), \tag{11}$$

$$\mathbf{P} = \int \mathbf{cc}^{\mathrm{T}} f d\mathbf{v}. \tag{12}$$

Here, the matrix $\mathbf{S}$ transforms a velocity $\mathbf{C}$ sampled from a Maxwellian distribution into a velocity $\mathbf{c}$ sampled from the ES distribution, the matrix $\mathbf{P}$ is the pressure tensor, and the matrix $\mathbf{I}$ is the identity tensor, all of which are symmetric.

As in the BGK model, the ES-BGK relaxation rate ν determines the viscosity μ and the thermal conductivity K according to the following expressions:[5–7]

$$\mu = \frac{nk_BT}{\nu}\mathrm{Pr}, \tag{13}$$

$$K = C_p\frac{nk_BT}{\nu}. \tag{14}$$

The ES-BGK expressions are identical to the analogous BGK expressions except for the factor of the Prandtl number in the viscosity, which allows the ES-BGK model to reproduce both the viscosity and the thermal conductivity simultaneously. In other words, the relaxation rate ν and the Prandtl number Pr are both inputs to the ES-BGK model. If the Prandtl number is chosen to be unity, the ES-BGK model becomes identical to the BGK model.

Holway[5–7] and Andries and co-workers[8–10] proposed extensions to the ES-BGK model that allow it to treat both gas mixtures and polyatomic molecules (i.e., molecules with internal degrees of freedom, such as rotation). Thus, in principle, the ES-BGK model can be applied to air, which is primarily a mixture of two diatomic molecules. Andries and co-workers[10] implemented their polyatomic ES-BGK model in a DSMC code and used it to simulate a flow of pure nitrogen. Herein, polyatomic molecules are not investigated, but mixtures of monatomic molecules are examined.

III. NUMERICAL IMPLEMENTATION

A. DSMC algorithm

The DSMC algorithm of Bird[21] uses molecular gas dynamics to represent noncontinuum gas flows. More specifically, computational molecules move, reflect from solid boundaries, and collide with each other in a pairwise fashion just as real gas molecules do. The move/reflect and collide portions of the algorithm are split into two distinct phases that are performed in alternating fashion. Herein, a fixed time step Δt that is small relative to the collision time scale t_0 is used for each phase. The computational mesh serves two purposes. First, collision partners are selected only from within the same mesh cell. Second, moments of the molecular velocity distribution are accumulated for each cell based on the properties of the molecules within that cell at each time step. Herein, a one-dimensional computational mesh with uniform cell size Δx that is small compared to the mean free path λ is used. However, it is emphasized that the molecules have three-dimensional velocities.

The variable-soft-sphere (VSS) model is used to represent molecular interactions.[21] This model depends on three parameters to determine the collision rate ν_0 (which is not the same as the ES-BGK relaxation rate ν): the viscosity temperature exponent ω, the angular scattering exponent α, and the reference molecular diameter d_{ref}. Hard-sphere interactions have $\omega=1/2$ and $\alpha=1$, whereas Maxwell interactions have $\omega=1$ and $\alpha=2.139\,86$. The reference diameter is given by the following expression, where "ref" denotes reference conditions:

$$d_{\mathrm{ref}}{}^2 = \frac{5(\alpha+1)(\alpha+2)(\mu_\infty/\mu_1)}{4\alpha(5-2\omega)(7-2\omega)\mu_{\mathrm{ref}}}\sqrt{\frac{mk_BT_{\mathrm{ref}}}{\pi}}. \tag{15}$$

Here, the quantity μ_∞/μ_1 is the infinite-to-first-approximation viscosity ratio from Chapman–Enskog theory (1.0160 34 for hard-sphere molecules and 1 for Maxwell molecules).[23–26] The corresponding collision rate is given by the following expression:

$$\nu_0 = 4d_{\mathrm{ref}}{}^2 n\sqrt{\frac{\pi k_B T_{\mathrm{ref}}}{m}}\left(\frac{T}{T_{\mathrm{ref}}}\right)^{1-\omega}. \tag{16}$$

The viscosity and the thermal conductivity have the following temperature dependence:

$$\frac{\mu}{\mu_{\mathrm{ref}}} = \frac{K}{K_{\mathrm{ref}}} = \left(\frac{T}{T_{\mathrm{ref}}}\right)^{\omega}. \tag{17}$$

The reference values of the thermal conductivity and the viscosity are related as follows:

$$\mathrm{Pr} = \frac{\mu C_p}{K} = \frac{\mu_{\mathrm{ref}} C_p}{K_{\mathrm{ref}}} = \frac{2}{3}\frac{\mu_\infty/\mu_1}{K_\infty/K_1}. \tag{18}$$

Here, directly analogous to the quantity μ_∞/μ_1, the quantity K_∞/K_1 is the infinite-to-first-approximation thermal-conductivity ratio from Chapman–Enskog theory (1.025 218 for hard-sphere molecules and 1 for Maxwell molecules).[23–26]

The Cercignani–Lampis–Lord (CLL) model is used to describe molecular reflections from solid boundaries.[27–29] Although the CLL model allows for quite general reflection processes, only unity values of the two accommodation coefficients are considered herein.

Moments of the molecular-velocity-distribution function are determined for each cell by sampling the properties of the molecules within each cell during every time step. Time averaging (during steady-state behavior) and ensemble averaging (typically 32 realizations) are both used to reduce stochastic uncertainty. To avoid bias in nonconserved moments, samples are acquired both before and after performing collisions. This approach has been shown to improve greatly the accuracy of cell-based moments of quantities that are not conserved in DSMC collisions.[30]

B. BGK and ES-BGK models

The BGK and ES-BGK kinetic models are also implemented using a molecular-gas-dynamics approach. Molecular movement, molecular reflection from solid boundaries, and sampling of molecular properties are performed in the same manner as in the DSMC algorithm. Only the (intracell) collision phase differs. The (constant) ratio of the ES-BGK relaxation rate ν to the DSMC VSS collision rate ν_0 given by Bird[21] is straightforwardly determined:

$$\frac{\nu}{\nu_0} = \frac{\alpha(5-2\omega)(7-2\omega)\mathrm{Pr}}{5(\alpha+1)(\alpha+2)(\mu_\infty/\mu_1)}. \tag{19}$$

The BGK-K model is obtained by using the BGK collision term [Eq. (4)] and by inserting the actual value of the Prandtl number in the relaxation-rate expression [Eq. (19)]. Similarly, the BGK-μ model is obtained by using the BGK collision term [Eq. (4)] but by inserting a value of unity for the Prandtl number in the relaxation-rate expression [Eq. (19)].

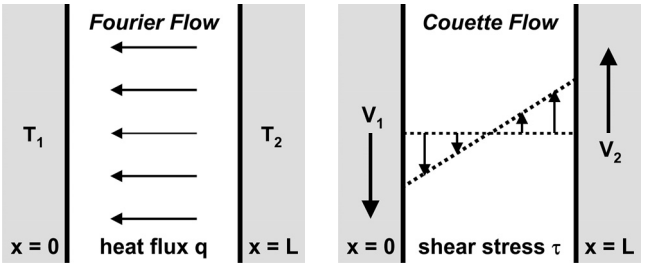

FIG. 1. Fourier and Couette flows.

Thus, the ES-BGK collision rate ν is determined for each cell at each time step from the corresponding VSS collision rate ν_0, which uses only properties of the molecules in that cell during that time step.[21] Calculating the relaxation rate in this way obviates the need to calculate macroscopic properties of the gas (such as temperature) that potentially could give rise to a random walk in the results.

The probability that any given molecule in the cell undergoes a relaxation is $P=1-\exp[-\nu\Delta t]$. Each molecule in the cell is assigned a random number uniformly distributed between zero and unity. If its random number is less than the relaxation probability, then a molecule is assigned a new thermal velocity drawn from the ES-BGK distribution, namely, Eqs. (9)–(12). After all molecules in the cell have been processed in this manner, their provisional postcollision velocities are adjusted to enforce conservation of momentum and energy at the cell level. The average velocity and the temperature of the molecules in a cell are determined for the precollision conditions ($\mathbf{u}$ and T) and for the provisional postcollision conditions ($\mathbf{u}_p$ and T_p). The final postcollision velocity $\mathbf{v}$ of every molecule (whether having undergone relaxation or not) is determined from these quantities and its provisional postcollision velocity $\mathbf{v}_p$ according to the following expression:

$$\mathbf{v} = \mathbf{u} + (\mathbf{v}_p - \mathbf{u}_p)\sqrt{T/T_p}. \tag{20}$$

This implementation differs slightly from that of Andries and co-workers,[8–10] who relaxed either all or none of the molecules within a cell based on whether a single random number uniformly distributed between zero and unity is either less than or greater than the relaxation probability. The cell-based approach is somewhat faster, but the molecule-based approach is more accurate within Knudsen layers near solid boundaries (e.g., as for the Fourier and Couette flows considered herein).

IV. FOURIER AND COUETTE FLOWS

A. Description

The ES-BGK, BGK-K, BGK-μ, and Boltzmann (DSMC) collision terms are used to perform molecular-gas-dynamics simulations of Fourier flow, Couette flow, and combined Fourier–Couette flow. Figure 1 shows schematic diagrams of Fourier and Couette flows. In these flows, gas is

TABLE I. Simulation parameters.

Quantity	Symbol	Value
Boltzmann constant	k_B	$1.380\,658\times10^{-23}$ J/K
Molecular mass	m	66.3×10^{-27} kg
Reference viscosity	μ_{ref}	2.117×10^{-5} Pa s
Reference temperature	T_{ref}	273.15 K
Reference pressure	p_{ref}	0.133 322 Pa=1 mTorr
Initial temperature	T_{init}	T_{ref}
Initial pressure	p_{init}	$(1-4000)p_{\text{ref}}$
Left wall temperature	T_1	$T_{\text{ref}}-\Delta T/2$
Right wall temperature	T_2	$T_{\text{ref}}+\Delta T/2$
Temperature difference	ΔT	0–400 K
Left wall velocity	V_1	$-\Delta V/2$
Right wall velocity	V_2	$+\Delta V/2$
Velocity difference	ΔV	0–100 m/s
Domain length	L	1 mm
Cell size	Δx	2.5 μm
Time step	Δt	7 ns
Molecules per cell	N_c	120

confined between two parallel solid walls that are separated by a distance L. The left wall is located at $x=0$ and has temperature $T_1=T_{\text{ref}}-\Delta T/2$ and tangential velocity $V_1=-\Delta V/2$, and the right wall is located at $x=L$ and has temperature $T_2=T_{\text{ref}}+\Delta T/2$ and tangential velocity $V_2=+\Delta V/2$. In Fourier flow, the walls are motionless ($\Delta V=0$) but are at different temperatures ($\Delta T\neq0$). In Couette flow, the walls are moving tangentially with equal but opposite velocities ($\Delta V\neq0$) but are at the same temperature ($\Delta T=0$). In combined Fourier–Couette flow, the walls are moving as in Couette flow and have different temperatures as in Fourier flow. Both walls have accommodation coefficients of unity.

The gas is taken to be argon, with molecular mass and reference viscosity from Bird.[21] However, as indicated above, the molecules collide according to either the Maxwell interaction ($\omega=1$ and $\alpha=2.139\,86$) or the hard-sphere interaction ($\omega=1/2$ and $\alpha=1$). Most molecular interactions are bounded by these two interactions, and many theoretical and computational results are available for them. Moreover, BGK-like models are most similar to the Maxwell interaction since they both have a rate that does not depend directly on the velocity of colliding molecules. Similarly, BGK-like models are least similar to the hard-sphere interaction, which has a collision rate that is proportional to the relative velocity of colliding molecules. Initially, the gas has pressure p_{init}, temperature T_{init}, and zero velocity everywhere in the domain. Ultimately, the gas achieves a statistically stationary (steady) nonuniform state throughout the domain.

Parameters used for all simulations are shown in Table I. The domain has a length of $L=1$ mm and is subdivided into 400 uniform cells with lengths of $\Delta x=2.5$ μm. Initially, each cell is filled with $N_c=120$ computational molecules having temperature $T_{\text{init}}=273.15$ K and pressure $p_{\text{init}}=1-4000$ mTorr, where 1 mTorr=0.133 322 Pa. At this temperature, the most probable molecular speed is $c_0=\sqrt{2k_BT/m}=337.3$ m/s. At the maximum pressure, the mean free path and the collision time scale are $\lambda=\sqrt{\pi}\mu c_0/2p=11.9$ μm and $t_0=\lambda/c_0=35.2$ ns. Thus, the normalized discretization parameters $\Delta x/\lambda$ and $\Delta t/t_0$ have values of 0.2 at the largest pressure and are proportional to the pressure. DSMC simulations under these conditions have been shown to produce highly accurate results.[30,31] Fourier flow has a temperature difference of $\Delta T=70$ K, Couette flow has a velocity difference of $\Delta V=100$ m/s, and combined Fourier–Couette flow has these temperature and velocity differences with additional simulations at temperature differences of $\Delta T=200$, 300, and 400 K. Time averaging after reaching steady state and ensemble averaging with 32 realizations are both used to reduce stochastic uncertainty.

B. Heat flux and shear stress

Figure 2 shows temperature and velocity profiles for Fourier flow at $\Delta T=70$ K and for Couette flow at $\Delta V=100$ m/s, respectively, which are obtained using the ES-BGK and Boltzmann collision terms for the Maxwell interaction with initial pressures of 2, 20, 200, and 2000 mTorr. At the lowest pressure, the profiles are nearly uniform and closely approach their corresponding free-molecular limits: $T_{\text{FM}}=\sqrt{T_1T_2}$ and $V_{\text{FM}}=0$. Similarly, at the highest pressure, the profiles are nearly linear with small jumps at the walls and closely approach their corresponding continuum limits, $T_C=\sqrt{T_1^2+(T_2^2-T_1^2)(x/L)}$ and $V_C\rightarrow\Delta V\{(x/L)-(1/2)\}$, in the limit of negligible viscous heating. The departure from linearity in the continuum temperature profile is caused by the temperature-dependent thermal conductivity. Similarly, the very small departure from linearity in the continuum velocity profile is caused by the combination of the temperature-dependent viscosity and the small temperature rise (less than 2 K) produced by viscous heating. In all cases, the ES-BGK kinetic model produces temperature and velocity profiles that are in good agreement with the corresponding profiles produced by the Boltzmann collision term. Although not shown, the temperature and velocity profiles produced by the BGK-K and BGK-μ kinetic models are also in reasonably good agreement because the profiles in the free-molecular limit are independent of the collision model by definition and the profiles in the continuum limit do not depend on the values of the viscosity and the thermal conductivity (as long as viscous heating is negligible).

Figure 3 shows the heat-flux and shear-stress values for these cases that are obtained using the ES-BGK, BGK-K, BGK-μ, and Boltzmann collision terms. As expected, all values are in excellent agreement in the free-molecular (low-pressure) limit because by definition collisions are negligible in this situation. For Fourier flow, the heat-flux values from the BGK-K, ES-BGK, and Boltzmann collision terms are all in good agreement and approach the continuum value, whereas the heat-flux values from the BGK-μ collision term lie systematically below the other values. Similarly, for Couette flow, the heat-flux values from the BGK-μ, ES-BGK, and Boltzmann collision terms are all in good agreement and approach the continuum value, whereas the heat-flux values from the BGK-K collision term lie systematically above the

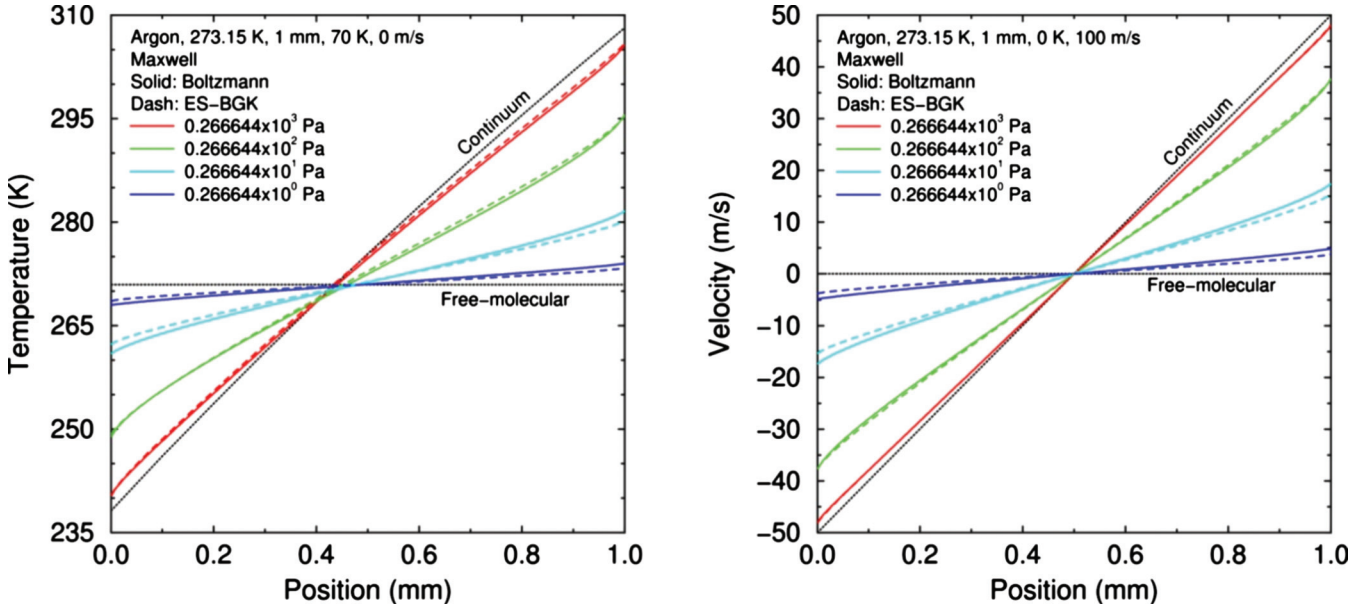

FIG. 2. (Color) Left: temperature profiles for Fourier flow. Right: velocity profiles for Couette flow.

other values. These trends illustrate the fact that the BGK model can reproduce either the thermal conductivity or the viscosity for a Prandtl number of around 2/3 but not both simultaneously. In the transitional (intermediate-pressure) regime, the ES-BGK collision term produces heat-flux and shear-stress values that are slightly higher than those produced by the Boltzmann collision term, with maximum differences of less than 3%. Thus, unlike the BGK-K and BGK-μ models, the ES-BGK model produces both heat-flux and shear-stress values that are in close agreement with the values produced by the Boltzmann collision term over the entire range of pressure.

Figure 4 shows the thermal-conductivity and viscosity profiles for Fourier flow and for Couette flow, respectively, for the above cases with initial pressures of 2000 mTorr. Here, the thermal conductivity and the viscosity have been normalized by their (temperature-dependent) Chapman–Enskog values, so values of unity should be obtained at continuum conditions. For Fourier flow, the BGK-K, ES-BGK, and Boltzmann collision terms yield thermal-conductivity ratios that are close to unity in the central region of the domain and that depart from unity in similar fashions in the Knudsen layers adjacent to the walls, whereas the BGK-μ collision term yields a significantly lower thermal-conductivity ratio in the central region. Similarly, for Couette flow, the BGK-μ, ES-BGK, and Boltzmann collision terms yield viscosity ratios that are close to unity in the central region of the domain and that depart from unity in similar fashions in the Knudsen

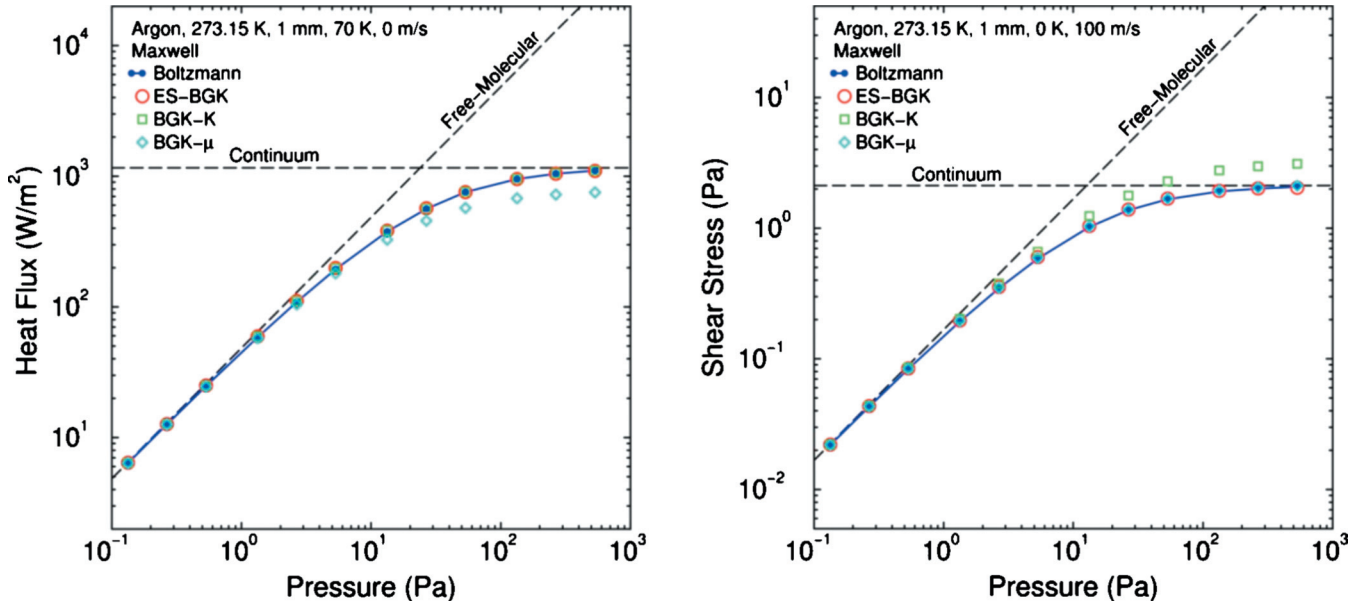

FIG. 3. (Color) Left: heat flux vs pressure for Fourier flow. Right: shear stress vs pressure for Couette flow.

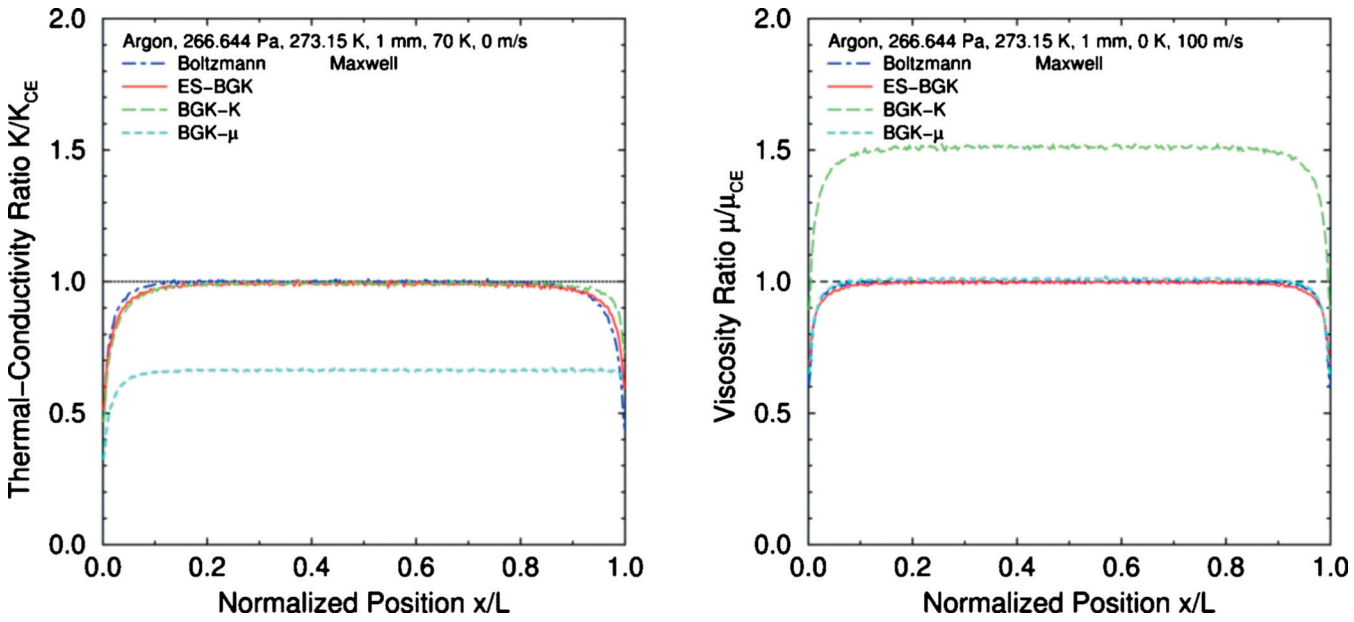

FIG. 4. (Color) Left: thermal-conductivity profiles for Fourier flow. Right: viscosity profiles for Couette flow.

layers adjacent to the walls, whereas the BGK-K collision term yields a significantly higher viscosity ratio in the central region. Interestingly, the ES-BGK collision term reproduces the behavior of the Boltzmann collision term in the Fourier-flow and Couette-flow Knudsen layers with similar accuracy to the BGK-K and BGK-μ collision terms, respectively. This behavior is similar to that observed by Garzó and Santos for uniform shear flow[19,20] and may be related to the fact that the CLL process for reflecting molecules from walls[27–29] produces a Maxwellian distribution, rather than an ellipsoidal-statistical distribution.

Figures 2–4 all show results based on using the Maxwell interaction to perform collisions. When the hard-sphere interaction is used instead, the temperature and velocity profiles and the corresponding heat-flux and shear-stress values at the pressures examined are virtually the same, so these results are not shown. This behavior is not surprising because the ES-BGK collision term is prescribed so as to yield correct values for the thermal conductivity and the viscosity. In Fig. 4, the left and right Knudsen layers of the thermal-conductivity and viscosity profiles are not mirror images because these transport properties depend on temperature, which varies across the domain by virtue of the wall boundary conditions and viscous heating in the bulk gas.

C. Velocity distribution function

As Cercignani observed,[1] the ES-BGK collision term approximates the collision process and thus may not reproduce higher-order moments of the molecular-velocity-distribution function accurately. The molecular-velocity-distribution function can be described using an expansion in Sonine polynomials.[23] The normalized coefficients of these polynomials, denoted as a_k/a_1 and b_k/b_1, where $k \geq 1$ is the index of the expansion, have been computed for both Maxwell and hard-sphere interactions in the small-perturbation continuum regime using infinite-approximation CE theory and for the Maxwell interaction in the finite-perturbation continuum regime using MH theory.[23–26] For $k \geq 2$, the CE values for the Maxwell interaction satisfy $a_k/a_1 = b_k/b_1 = 0$, whereas the CE values for the hard-sphere interaction satisfy $a_k/a_1 > b_k/b_1 > 0$. Thus, these normalized coefficients provide sensitive measures of the precise shape of the molecular-velocity-distribution function.

As with other physical quantities, the Sonine-polynomial-coefficient ratios are functions of moments of the molecular velocity distribution f. In a molecular-gas-dynamics algorithm, these moments are determined just like any other moments by sampling the properties of molecules within each cell during each time step. Previous DSMC simulations of combined Fourier–Couette flow using the Boltzmann collision term have reproduced the Maxwell and hard-sphere CE theoretical values and the Maxwell MH theoretical values to high accuracy.[24–26] Corresponding molecular-gas-dynamics simulations of combined Fourier–Couette flow are performed herein using the ES-BGK collision term. In all cases, the initial gas temperature is $T_{\text{init}} = 273.15$ K, the initial gas pressure is $p_{\text{init}} = 2000$ mTorr, the wall velocity difference is $\Delta V = 100$ m/s, and the gas has the molecular mass and reference viscosity of argon.

Figures 5 and 6 show the Sonine-polynomial-coefficient ratios a_k/a_1 and b_k/b_1 for the Maxwell and hard-sphere interactions, respectively, which are obtained using the ES-BGK and Boltzmann collision terms. The wall temperature difference for these simulations is $\Delta T = 70$ K, which is small enough for the CE theoretical values to be obtained outside of the Knudsen layers (i.e., in the central region of the domain). As indicated above, the Boltzmann collision term reproduces the CE theoretical values in the central region for both the Maxwell interaction and the hard-sphere interaction. However, the ES-BGK collision term does not closely reproduce the CE values and does not even produce

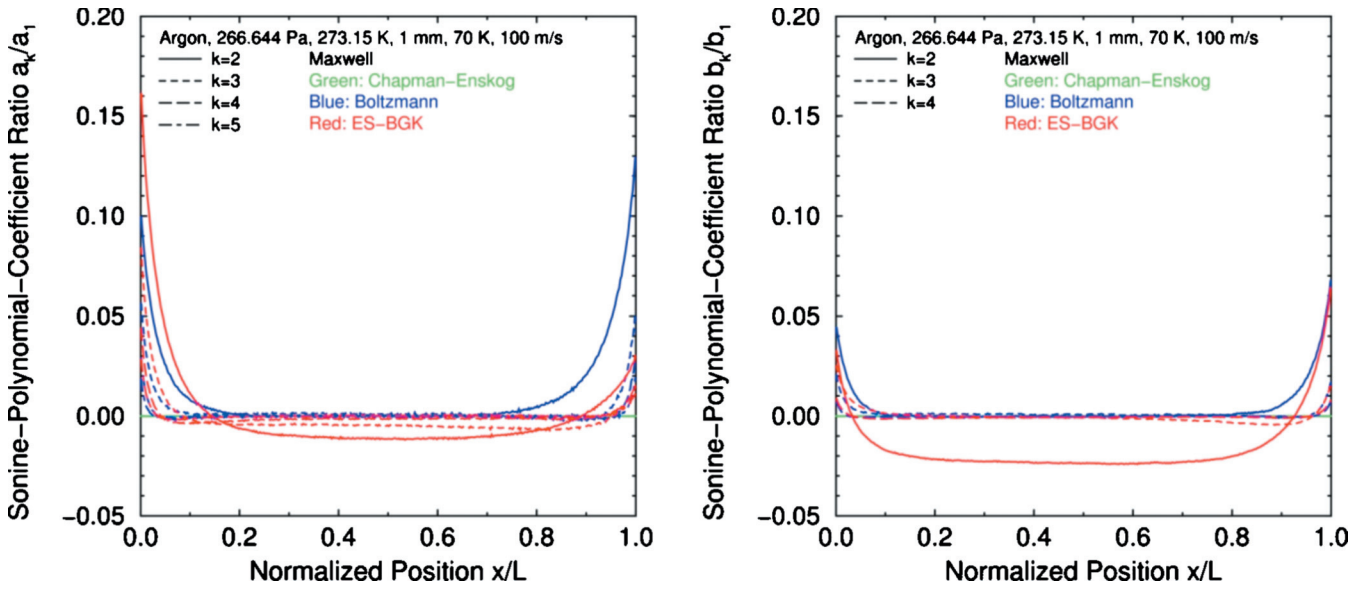

FIG. 5. (Color) Sonine-polynomial-coefficient profiles for Fourier–Couette flow with the Maxwell interaction.

values that are spatially uniform in the central region. Instead, unlike the Boltzmann collision term, the ES-BGK collision term produces similar values for the Maxwell and hard-sphere interactions, and these values are all small on the scale of the CE hard-sphere values. Hence, for both interactions, the ES-BGK collision term produces molecular velocity distributions that are much more similar to those produced by the Maxwell interaction than to those produced by the hard-sphere interaction. This behavior is reasonable given that the ES-BGK collision term uses a relaxation rate that does not directly depend on the molecular velocity and that the Boltzmann collision term with the Maxwell interaction similarly produces a collision rate that does not depend on the relative velocity of the colliding pair.

Figure 7 shows the first few Sonine-polynomial-coefficient ratios for the Maxwell interaction that are obtained using the ES-BGK and Boltzmann collision terms for finite values of the heat flux. These values are determined from the solutions obtained for four distinct wall temperature differences: $\Delta T = 70$, 200, 300, and 400 K. The Sonine-polynomial-coefficient ratios are plotted against the heat-flux Knudsen number, where q is the heat flux:

$$\mathrm{Kn}_q = q/mnc_0^3. \tag{21}$$

Although the heat flux is spatially uniform throughout the domain, the heat-flux Knudsen number varies with position even in the central region of the domain, because it is approximately inversely proportional to the square root of the temperature. Therefore, a single simulation provides a range of values for the heat-flux Knudsen number and a corresponding range of values for the Sonine-polynomial-

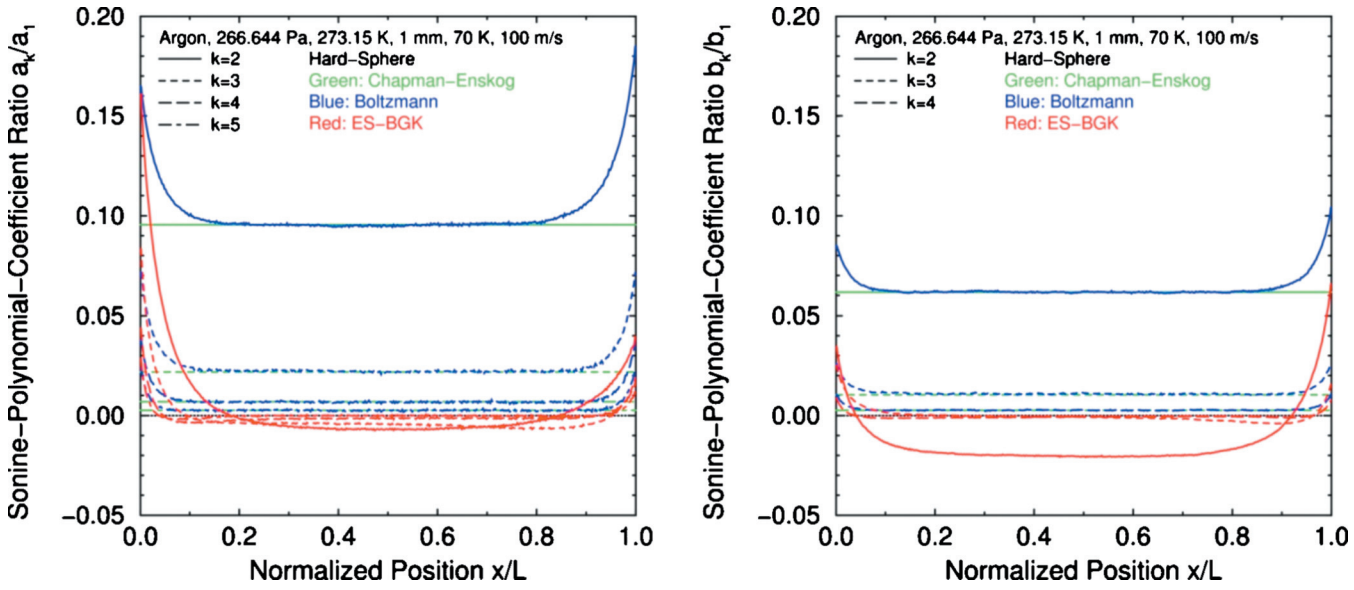

FIG. 6. (Color) Sonine-polynomial-coefficient profiles for Fourier–Couette flow with the hard-sphere interaction.

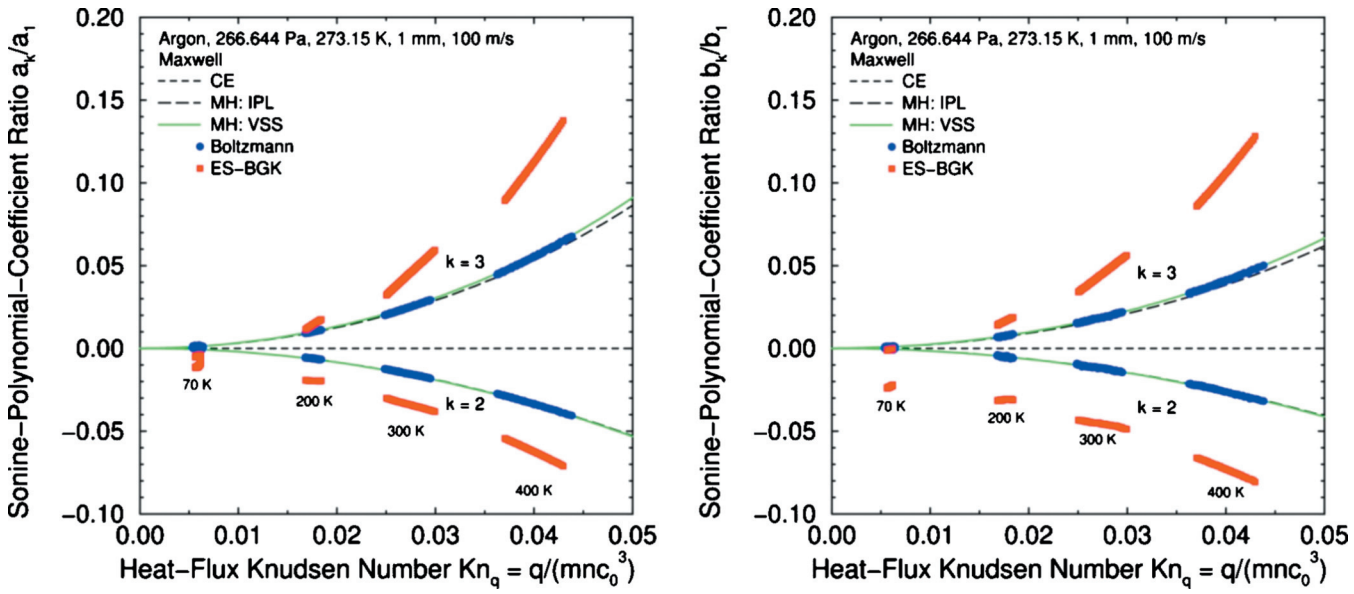

FIG. 7. (Color) Sonine-polynomial-coefficient values vs heat-flux Knudsen number for Fourier–Couette flow with the Maxwell interaction.

coefficient ratios. The MH theoretical values for both the Maxwell-VSS interaction (used by the DSMC algorithm) and the Maxwell-IPL interaction (which represents an inverse-power-law intermolecular force) are also shown. As previously observed,[24–26] the Boltzmann collision term with the Maxwell-VSS interaction as implemented in the DSMC algorithm closely reproduces the corresponding MH values. While behaving in a qualitatively similar fashion, the ES-BGK-values differ from the MH values by order-unity amounts. Thus, the ES-BGK collision term produces even less accurate molecular-velocity-distribution functions for larger departures from equilibrium (e.g., large heat fluxes). This effect is expected to be more important for higher-order terms and for higher Knudsen numbers.

D. Mass self-diffusion

The ES-BGK and Boltzmann (DSMC) collision terms can also be used to perform molecular-gas-dynamics simulations of Fickian diffusion. The geometry is the same as for Fourier and Couette flows, shown in Fig. 1. In Fickian diffusion, gas is confined between two parallel isothermal motionless solid walls. The left and right walls have temperature $T_1=T_2=T_{\text{ref}}$ and tangential velocity $V_1=V_2=0$ (i.e., $\Delta T=0$ and $\Delta V=0$). As in previous simulations, the gas is taken to be argon except that the molecules collide according to either the Maxwell interaction or the hard-sphere interaction. Initially, the gas has pressure p_{init}, temperature $T_{\text{init}}=T_{\text{ref}}$, and velocity $u=0$ everywhere in the domain. At all subsequent times, the gas remains in this statistically stationary (steady) uniform state throughout the domain. As for previous simulations, Table I shows the parameters used for these simulations.

To observe mass self-diffusion, all molecules are tagged as either type 1 or type 2, with half of the molecules initially assigned to each type. The tags of all molecules reflecting from the left wall are reassigned to type 1, and the tags of all molecules reflecting from the right wall are reassigned to type 2. Molecular movements and collisions are performed in a manner that is independent of the molecule type, but statistical quantities such as number density and number flux are collected separately for each type. It is emphasized that type 1 and type 2 molecules are dynamically indistinguishable: The molecule type is a completely passive tag.

Figure 8 shows the steady profiles of number density and velocity (the ratio of number flux to number density) for each type that are obtained with the Maxwell interaction. The type conversions at the walls create equal and opposite gradients in the number densities n_1 and n_2 and equal and opposite number fluxes n_1u_1 and n_2u_2, although the total number density $n=n_1+n_2$ is uniform in space and the total number flux $nu=n_1u_1+n_2u_2$ is zero everywhere.

The computed mass self-diffusion coefficient D is determined by inserting the computed number densities n_i and number fluxes n_iu_i into Fick's law:[23]

$$n_iu_i = -D\frac{\partial n_i}{\partial x}, \quad i=1,2. \tag{22}$$

The theoretical mass self-diffusion coefficient D_{CE} is determined from Chapman-Enskog theory for the Maxwell and hard-sphere interactions as below:[23–26]

$$\frac{D_{\text{CE}}}{\mu/\rho} = \frac{D_\infty/D_1}{\mu_\infty/\mu_1}\frac{3(3\nu-5)}{5(\nu-1)}\frac{A_2[\nu]}{A_1[\nu]}. \tag{23}$$

Here, D_∞/D_1 is the infinite-to-first approximation ratio of the mass self-diffusion coefficient (1.0189 54 for hard-sphere molecules and 1 for Maxwell molecules), $A_1[\nu]$ and $A_2[\nu]$ are functions tabulated by Chapman and Cowling, $\nu=1+4/(2\omega-1)$ (∞ for hard-sphere molecules and 5 for Maxwell molecules), and $\rho=mp/k_BT$ is the mass density. For the conditions considered herein, the following values are obtained: 0.007 003 00 m^2/s for Maxwell molecules and 0.005 434 89 m^2/s for hard-sphere molecules.

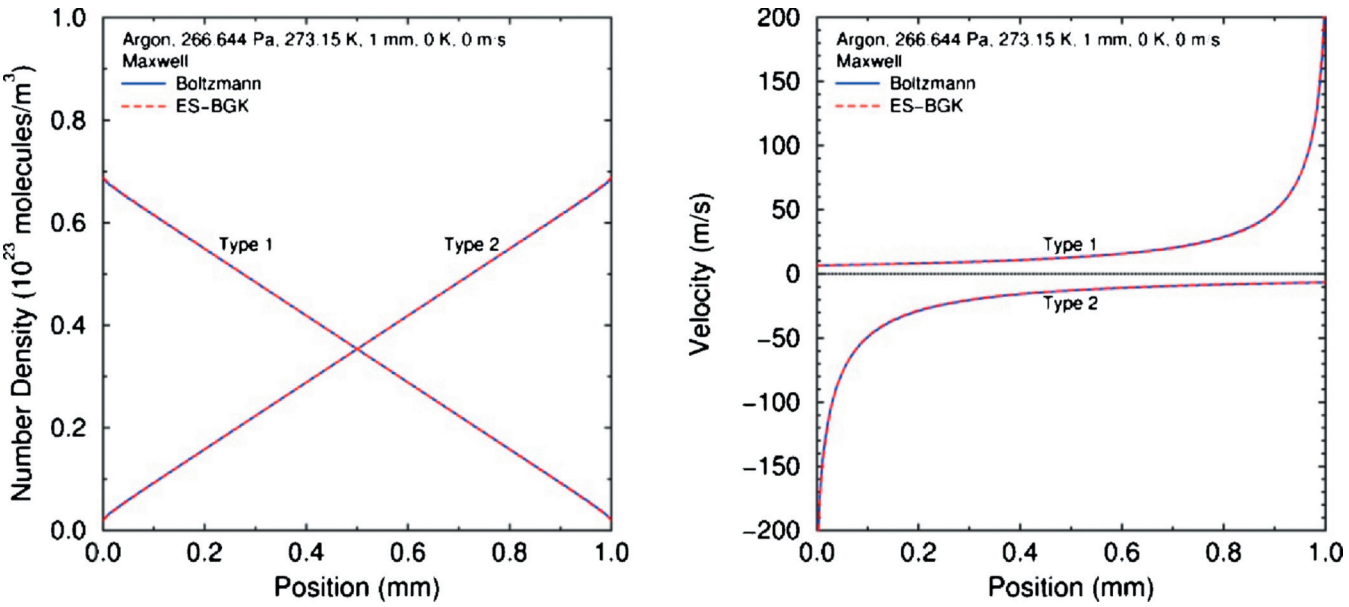

FIG. 8. (Color) Fickian diffusion with the Maxwell interaction. Left: number-density profiles. Right: velocity profiles.

Figure 9 shows the steady profiles of the ratio of the computed and theoretical mass self-diffusion coefficients for the Maxwell and hard-sphere interactions. As for Fourier and Couette flows, Knudsen layers are seen adjacent to the walls. Although the Boltzmann collision term reproduces the CE theoretical value accurately in the central region of the domain for both interactions, the ES-BGK collision term fails to do so, producing values that are 2% too small for the Maxwell interaction and 28% too large for the hard-sphere interaction.

V. CONCLUSIONS

As Cercignani succinctly asserted,[1] simple kinetic models that ignore the fine details of molecular collisions can accurately reproduce some macroscopic properties of a gas flow. This assertion has been assessed herein for the ES-BGK kinetic model, proposed originally by Holway[5–7] and popularized early on by Cercignani and Tironi.[14] Unlike the earlier BGK kinetic model, the ES-BGK kinetic model provides accurate values of both the heat flux and the shear stress at all pressures for gas confined between two parallel walls (i.e., combined Fourier–Couette flow).

Not surprisingly, the ES-BGK kinetic model does not do as well in predicting the shape of the molecular-velocity-distribution function. Instead, the ES-BGK kinetic model produces molecular-velocity-distribution functions that are similar to those produced by the Maxwell interaction regardless of the particular interaction ostensibly represented by the

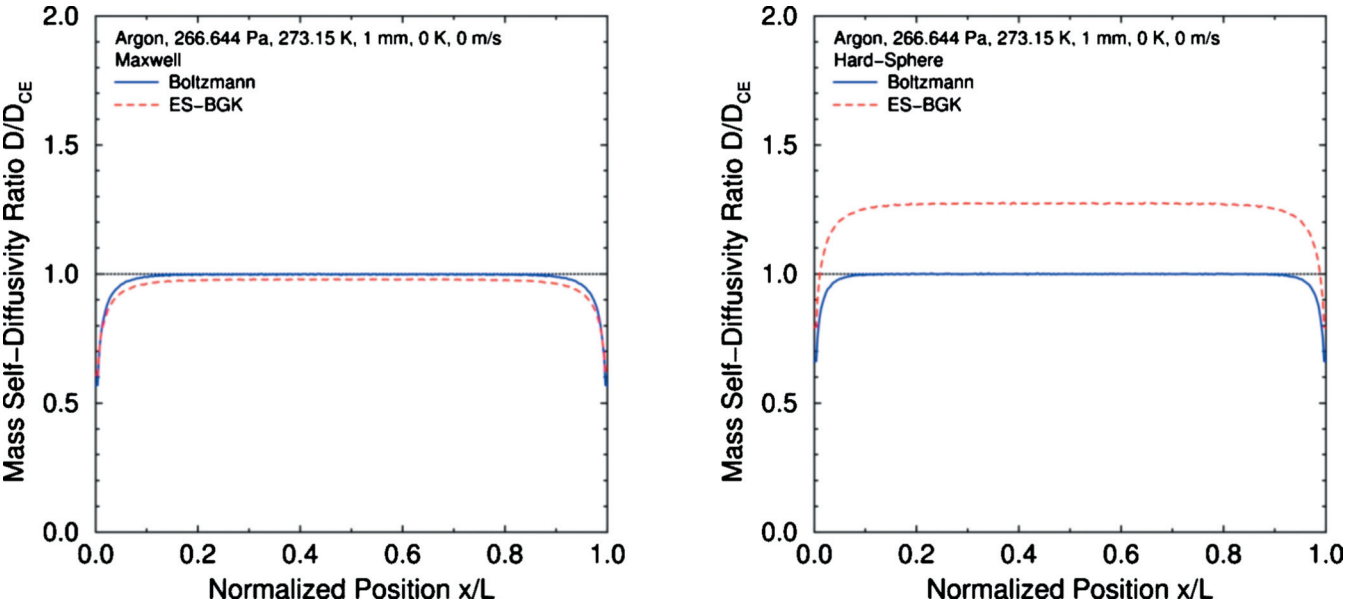

FIG. 9. (Color) Mass self-diffusivity profiles for Fickian diffusion. Left: Maxwell interaction. Right: hard-sphere interaction.

ES-BGK kinetic model (e.g., hard sphere). This behavior is reasonable given that both the ES-BGK model and the Maxwell interaction involve rates that do not depend directly on the molecular velocity.

Similarly, the ES-BGK model does not do well in predicting mass-diffusion phenomena. More specifically, the ES-BGK values of the mass self-diffusion coefficient differ significantly from the theoretical values for the Maxwell and hard-sphere interactions. Since thermal diffusion in a gas mixture depends strongly on the molecular interaction (it is zero for Maxwell and maximum for hard sphere),[32] simulating this flow would provide an even more sensitive test.

ACKNOWLEDGMENTS

Sandia National Laboratories is a multi-program laboratory managed and operated by Sandia Corporation, a wholly owned subsidiary of Lockheed Martin Corporation, for the U.S. Department of Energy's National Nuclear Security Administration under Contract No. DE-AC04-94AL85000.

[1] C. Cercignani, *The Boltzmann Equation and Its Applications* (Springer-Verlag, New York, 1988), Chap. II, Sec. 10.
[2] H. Struchtrup, *Macroscopic Transport Equations for Rarefied Gas Flows: Approximation Methods in Kinetic Theory* (Springer-Verlag, Berlin, 2005).
[3] P. L. Bhatnagar, E. P. Gross, and M. Krook, "A model for collision processes in gases. I. Small amplitude processes in charged and neutral one-component systems," Phys. Rev. **94**, 511 (1954).
[4] W. G. Vincenti and C. H. Kruger, Jr., *Introduction to Physical Gas Dynamics* (Wiley, New York, 1965).
[5] L. H. Holway, Jr., "Approximation procedures for kinetic theory," Ph.D. thesis, Harvard University, 1963.
[6] L. H. Holway, Jr., "Kinetic theory of shock structure using an ellipsoidal distribution function," in *Rarefied Gas Dynamics: Proceedings of the Fourth International Symposium*, edited by J. H. de Leeuw (Academic, New York, 1965), Vol. 1, pp. 193–215.
[7] L. H. Holway, Jr., "New statistical models for kinetic theory: Methods of construction," Phys. Fluids **9**, 1658 (1966).
[8] P. Andries, P. le Tallec, J.-P. Perlat, and B. Perthame, "The Gaussian-BGK model of Boltzmann equation with small Prandtl number," Eur. J. Mech. B/Fluids **19**, 813 (2000).
[9] P. Andries and B. Perthame, "The ES-BGK model equation with correct Prandtl number," in *Rarefied Gas Dynamics: Proceedings of the 22nd International Symposium*, edited by T. J. Bartel and M. A. Gallis (American Institute of Physics, Melville, NY, 2001), Vol. 585, pp. 30–36.
[10] P. Andries, J.-F. Bourgat, P. le Tallec, and B. Perthame, "Numerical comparison between the Boltzmann and ES-BGK models for rarefied gases," Comput. Methods Appl. Mech. Eng. **191**, 3369 (2002).
[11] H. W. Liepmann, R. Narasimha, and M. T. Chahine, "Structure of a plane shock layer," Phys. Fluids **5**, 1313 (1962); "Erratum: Structure of a plane shock layer [Phys. Fluids 5, 1313 (1962)]," **8**, 551 (1965).
[12] B. M. Segal and J. H. Ferziger, "Shock-wave structure using nonlinear model Boltzmann equations," Phys. Fluids **15**, 1233 (1972).
[13] M. A. Gallis and J. R. Torczynski, "The application of the BGK model in particle simulations," AIAA Paper No. 2000-2360, 2000.
[14] C. Cercignani and G. Tironi, "Nonlinear heat transfer between two parallel plates at large temperature ratios," in *Rarefied Gas Dynamics: Proceedings of the Fifth International Symposium*, edited by C. L. Brundin (Academic, New York, 1967), Vol. 1, pp. 441–453.
[15] A. A. Alexeenko, E. P. Muntz, M. A. Gallis, and J. R. Torczynski, "Comparison of kinetic models for gas damping of moving microbeams," AIAA Paper No. 2006-3715, 2006.
[16] S. Chigullapalli, A. Venkattraman, and A. A. Alexeenko, "Modeling of viscous shock tube using ES-BGK model kinetic equations," AIAA Paper No. 2009-1317, 2009.
[17] Z.-H. Li and H.-X. Zhang, "Gas-kinetic numerical studies of three-dimensional complex flows on spacecraft re-entry," J. Comput. Phys. **228**, 1116 (2009).
[18] N. Gimelshein, S. Gimelshein, N. Selden, and A. Ketsdever, "Modeling of low-speed rarefied gas flows using a combined ES-BGK/DSMC approach," Vacuum **85**, 115 (2010).
[19] V. Garzó and A. Santos, "Comparison between the Boltzmann and BGK equations for uniform shear flow," Physica A **213**, 426 (1995).
[20] V. Garzó and A. Santos, *Kinetic Theory of Gases in Shear Flows: Nonlinear Transport* (Kluwer Academic, Dordrecht, 2003).
[21] G. A. Bird, *Molecular Gas Dynamics and the Direct Simulation of Gas Flows* (Clarendon, Oxford, 1994).
[22] W. Wagner, "A convergence proof for Bird's direct simulation Monte Carlo method for the Boltzmann equation," J. Stat. Phys. **66**, 1011 (1992).
[23] S. Chapman and T. G. Cowling, *The Mathematical Theory of Non-Uniform Gases*, 3rd ed. (Cambridge University Press, Cambridge, England, 1970).
[24] M. A. Gallis, J. R. Torczynski, and D. J. Rader, "Molecular gas dynamics observations of Chapman-Enskog behavior and departures therefrom in nonequilibrium gases," Phys. Rev. E **69**, 042201 (2004).
[25] J. R. Torczynski, M. A. Gallis, and D. J. Rader, "DSMC simulations of Fourier and Couette flow: Chapman-Enskog behavior and departures therefrom," in *Rarefied Gas Dynamics: 24th International Symposium*, edited by M. Capitelli (American Institute of Physics, Melville, NY, 2005), Vol. 762, pp. 620–625.
[26] M. A. Gallis, J. R. Torczynski, D. J. Rader, M. Tij, and A. Santos, "Normal solutions of the Boltzmann equation for highly nonequilibrium Fourier flow and Couette flow," Phys. Fluids **18**, 017104 (2006).
[27] C. Cercignani and M. Lampis, "Kinetic models for gas-surface interactions," Transp. Theory Stat. Phys. **1**, 101 (1971).
[28] R. G. Lord, "Some extensions to the Cercignani-Lampis gas-surface scattering kernel," Phys. Fluids A **3**, 706 (1991).
[29] R. G. Lord, "Some further extensions of the Cercignani-Lampis gas-surface scattering kernel," Phys. Fluids **7**, 1159 (1995).
[30] D. J. Rader, M. A. Gallis, J. R. Torczynski, and W. Wagner, "DSMC convergence behavior of the hard-sphere-gas thermal conductivity for Fourier heat flow," Phys. Fluids **18**, 077102 (2006).
[31] M. A. Gallis, J. R. Torczynski, D. J. Rader, and G. A. Bird, "Convergence behavior of a new DSMC algorithm," J. Comput. Phys. **228**, 4532 (2009).
[32] K. E. Grew and T. L. Ibbs, *Thermal Diffusion in Gases* (Cambridge University Press, Cambridge, England, 1952).